SciEn
Journal of Engineering Advancements Vol. 03(01) 2022, pp 029-041 https://doi.org/10.38032/jea.2022.01.005

Fundamental Study of CH_4-Air Combustion under an Axisymmetric Small-scale Rectangular Combustor using Computational Modeling

Karan Gaglani[1], *Md. Amzad Hossain*[2,*]

[1]Department of Aerospace Engineering, Embry-Riddle Aeronautical University, Prescott, AZ-86301, USA
[2]Department of Mechanical Engineering, Embry-Riddle Aeronautical University, Prescott, AZ-86301, USA

Received: February 13, 2022, Revised: March 25, 2022, Accepted: March 25, 2022, Available Online: March 28, 2022

ABSTRACT

The optimization of the design and operating conditions of industrial combustors depends on the fundamental study of combustion dynamics and flow behaviors. Complete combustion increases the thermal efficiency as well as reduces the emission significantly. A study of this kind also allows exploring alternative fuels that would increase the combustion efficiency thus the life cycle of the systems. To develop a highly-performed combustion system for power plants and/or rocket engines, fundamental research under an axisymmetric small-scale combustor is considered in this study. The k-ε (2 Eqn.) and species transport model (STM) are used to study the flow turbulence and combustion behavior, respectively. A Parallel flow injection configuration of fuel and air is considered. Combustion behavior is investigated at a wide range of fuel and air flow rate conditions while keeping the air slot dimension (240 mm) and fuel injection slot diameter (10 mm) constant. The fuel velocity (FV) and air velocity (AV) are changed from 2 m/s to 30 m/s so that a better test matrix could be proposed. At each run, turbulence, the flame temperature, reaction heat release rate, mass fraction of CO_2, etc are studied. It is seen that the combustion temperature increases with the increase in fuel injection velocity. The static flame temperature varies from 1855 K (min.) to 2350 K (max.) and falls within the standard limits of CH_4-Air combustion. The mass fraction of CO_2 is found to be within the acceptable limit (0.121 to 0.153). The heat of the reaction changes from 1.2 W (min.) to 15.6 W (max.) at variable Re_{air} and Re_{CH4} conditions. It is observed that the computational models used in this study are capable of predicting the flow and combustion behaviors accurately.

Keywords: Axisymmetric Combustor, Parallel Flow Injection, Species Transport Model, Flame Temperature, Heat of Reaction, Emission.

1 Introduction

Combustion is a chemical reaction in which different forms of energy are produced. Daily, the amount of CO_2 released is increasing. Thus research is being done to make the combustion processes more efficient to lower their impact on the environment. The US has been showing a trending growth in oil demand followed by China [1]. According to the International Energy Association (IEA, 2020 Edition) [1], the US had produced a 5.41GT (Gigaton) of CO_2 in 2018. The US had experienced an increase of ~ 3% unlike the European Union and Japan which have continued the decline. Therefore, the fundamental study of combustion is crucial for the development of clean energy technologies for power plants, airplane industries, rockets, etc.

Researchers have been doing extensive research developing highly-performed combustors and green combustion technologies. There is a lot of experimental and CFD research on premixed and non-premixed combustion. For example, Hossain et al. [2]-[5] have performed laser diagnostics (PLIF and PIV) and premixed combustion modeling to understand the flow and flame interaction at a wide range of Reynolds numbers and equivalence ratio conditions. They have developed the flame front tracing tools and developed optimum operating conditions for lab-scale high-speed combustion tests. Hamzah [6] compared the combustion performance of propane and methane inside an axial combustor using a non-premixed combustion model. They showed that the maximum temperature for propane is less than the methane and NO_x production is mostly controlled by the temperatures. Ibrahim [7] studied the effect of radiation on the flame size and overall flame performance in a methane-air combustion medium. They found that the air swirl number and the combustor exit to Swirler diameter ratio adversely influenced the flame temperature and flame length. Pitsch et al. [8] have performed a flamelet formulation model and investigated the effect of exact differential diffusion on the flame performance. They showed that the accurately measured Lewis number could be used to predict the scalar dissipation rate, pressure, and boundary conditions. Matalon et al. [9] have investigated the combustion instabilities in both premixed and non-premixed combustion. They studied the role of different types of diffusion, thermal expansion, and heat losses on flame instabilities. They showed that the instabilities in premixed combustion are mostly controlled by the thermal expansion, whereas, in diffusion (non-premixed) flame, instabilities are controlled by the thermal-diffusive effects. Lacaze et al. [10] have performed non-premixed combustion based on the flame structure analysis. They have investigated the flame stability in a liquid rocket engine near critical and supercritical conditions. They found that the flame stability is greatly controlled by the pressure, local strain, and temperature variations. Barths et al [11] have investigated the combustion performance of direct injection diesel engines using flamelet-based non-premixed combustion modeling. They proved that the multiple flamelets model (MFM) improves the understanding of the ignition phase, combustion pressure, heat release, and emission characteristics.

*Corresponding Author Email Address: hossaim4@erau.edu
Published by: SciEn Publishing Group

Hossain et al. [12] have studied the effect of Ultra Low-swirl Burner (LSB) (S = 0.17) on the combustion behavior of non-premixed methane-air mixture at low-to-high Re conditions. It was seen that the swirl number and Re play a significant role in combustion stability and thermal performance.

Although there are enormous scientific resources on non-premixed combustion, the applicability of those models is severely limited. In non-premixed combustion, the mass fractions are assigned in the model. There is no control over combustion reactions or combustion kinetics. Therefore, how species are generated, transformed through the combustion process, and how the diffusion controls the chemical kinetics can not be entirely explained by the non-premixed (NPM) combustion model. It is the species transport model (STM) that provides more information on species-derived chemical kinetics of the combustion. However, the scholarly resources on species transport model (STM)-based combustion are very limited, especially those for industrial applications. For example, Kassem et al. [13] have utilized the eddy dissipation model along with the species transport equations and studied the turbulent combustion of methane-jet flame. They showed that the ANSYS fluent overpredicts the flame mean temperature and underpredicts the flame length at the centerline of the combustor. Kongre et al. [14] have performed CFD and experimental tests to validate the combustion behavior of a direct ignition diesel engine.

Furthermore, the scientific resources on the design and optimization of industrial combustors are very limited. For example, Enagi et al. [15] have used the species transport model and non-premixed combustion model with laminar finite rate technique. They have optimized the design and performance criterion of the combustor. Davis et al. [16] have developed a comprehensive kinetic model to accurately predict H_2-CO combustion data. D'Errico et al. [17] performed CFD modeling to design and optimize the combustion system for modern heavy-duty diesel engines. The information regarding the safe experimental methodology, optimum operating conditions, or test matrix is still limited. Hossain et al. [18] have studied the fundamentals of CH_4-Air combustion in a cross-flow configuration under a small-scale combustor using the STM. The diffusion flame and its interaction with flow characteristics were studied at limited operating conditions. A more fundamental combustion study needs to be done to develop a next-generation highly-performed combustor for the industry.

To address the above issues, the species transport model (STM) is used to study the CH_4-Air combustion under an axisymmetric small-scale combustor. The combustion is performed at equivalence ratio (ϕ) = 1.0 and a wide range of CH_4 and Airflow conditions. The global combustion characteristics such as static flame temperatures, heat release rates, and mass fraction of CO_2 are investigated. Flow characteristic such as turbulent Intensity (I) is also measured. A relation has been made between the combustion and flow characteristics at a wide range of methane and airflow velocities. The ongoing work aims to optimize the test operating conditions of the proposed axisymmetric combustor.

2 Computational Methodology

For this study, a combustor with a length of 1800 mm and a width of 250 mm is examined. The authors come up with these dimensions based on the findings of previous research articles which could be found elsewhere [18]. As illustrated in Fig. 1, the fuel and air injection holes both are accommodated within the width of the combustor. The test operating conditions are optimized by maintaining the fuel slot height at 10 mm and the air slot height at 240 mm. The surface mesher and smooth transition inflation are used to create the mesh. Mesh Independence study is carried out by refining the grid size, grid growth rate, grid aspect ratios, etc. Based on the CFD analysis, going over mesh elements of 203424 and nodes of 204330 does not significantly affect the flow and flame characteristics. Considering the mesh independence study, the authors decided to use the mesh elements of 203424 and nodes of 204330 for this research (Fig. 2).

Fig. 1 2D Axisymmetric Combustor

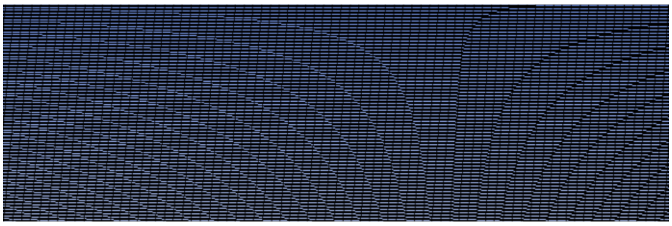

Fig. 2 The Meshing Domain

To discretize the fluid flow governing equations, the finite volume method (FVM) is utilized. A pressure-based, absolute, steady, and 2D axisymmetric space is considered in this study. The Energy equation and volumetric reaction are turned ON. Standard k-ε (2 Eqn.) and species transport equation are used for turbulence and combustion study. For the k and ε [18], the following two transport equations are used:

$$\frac{\partial}{\partial t}(\rho k)+\frac{\partial}{\partial x_i}(\rho k u_i)=\frac{\partial}{\partial x_j}\left[\left(\mu+\frac{\mu}{\sigma_k}\right)\frac{\partial k}{\partial x_j}\right]+G_k+G_b+\rho\varepsilon-Y_M+Y_k \qquad (1)$$

$$\frac{\partial}{\partial t}(\rho\varepsilon)+\frac{\partial}{\partial x_j}(\rho\varepsilon u_i)=\frac{\partial}{\partial x_i}\left[\left(\mu+\frac{\mu_t}{\sigma_\varepsilon}\right)\frac{\partial k}{\partial x_j}\right]+C_{1\varepsilon}\frac{\varepsilon}{k}(G_k+C_{2\varepsilon}G_b)-C_{2\varepsilon}\rho\frac{\varepsilon^2}{k}+S\varepsilon \qquad (2)$$

Where, G_k and G_b are the turbulent kinetic energy (TKE) generation due to the average velocity gradient and buoyancy forces, respectively, μ_t is the turbulent viscosity, and μ is the molecular viscosity. The source terms used for the energy transport phenomena are σ_k and $S\mathcal{E}$. The Y_M term in the k equation shows the contribution of fluctuating dilation to the overall dissipation rate. In the ε equation, $C_{1\varepsilon}$, $C_{2\varepsilon}$ and $C_{3\varepsilon}$ are the volume fraction constants and $S\mathcal{E}$ is the user-defined source terms.

The species transport model (STM) is used to account for the effect of chemical reactions and the nature of components and species. The general equation for the species transport model is expressed below [18]-[19],

$$\frac{\partial}{\partial t}(\rho Y_i)+\nabla.(\rho\vec{v}Y_i)=-\nabla.\vec{J_i}+R_i+S_i \qquad (3)$$

Where $\vec{J_i}$ is the diffusion flux of species i due to the change in concentration and temperature gradients, R_i is the net rate of production of species i by the chemical reaction, Y_i is the local mass fraction of species, S_i is the rate of creation by additional sources such as particulate, soot, emission, etc. The R_i is determined by Eddy-Dissipation Model (EDM). The details about EDM could be found elsewhere [18]. The following equation is used to predict the mass diffusion in a turbulent flow,

$$\vec{J_i} = -\left(\rho D_{i,m} + \frac{\mu_t}{Sc_t}\right) \nabla Y_i - D_{T,i} \frac{\nabla T}{T})[Turbulent\ Flow] \qquad (4)$$

Where $D_{T,i}$ is the thermal diffusion coefficient, $D_{i,m}$ is the mass diffusion coefficient, Sc_t is the turbulent Schmidt number, D_t is the turbulent diffusivity. The detail of those models could be found in [12], [18]-[20]. The boundary conditions and solution schemes used for this study are listed in Table 1 and Table 2.

Table 1 The Boundary Conditions Used in STM

Parameters	Conditions/Ranges
Equivalence Ratio (ϕ)	1.0 [Stoichiometric Condition]
Wall	Stationary Wall with Standard Wall Roughness
Outlet	Pressure Outlet
Re_{CH4}	1.2 E+3 to 1.2 E+4
Re_{Air}	3.2 E+4 to 3.2 E+5

Table 2 The Solution Schemes Used in STM

Parameters	Solution Schemes
Solution Initialization	Hybrid Initialization
Scheme Used	Couple
Spatial Discretization	Pressure: Second Order Momentum/TKE/TDR/CH_4/O_2/CO_2/H_2O/ Energy: Second-Order Upwind

3 Numerical Uncertainties and Validation

The numerical uncertainties are calculated to see how off the results are from the true value (target). The variable input values are implemented to measure the numerical sensitivity. The repeated measurements are performed to characterize the random (precision) uncertainty. The overall uncertainty varies between 0.05% and 0.90%. The calculated numerical uncertainties fall within the acceptable standard limits of uncertainties (≤5%). Thus, the results presented in this paper are deemed to be valid. The numerical uncertainty is listed in Table 3.

Table 3 The Numerical Uncertainties in Computational Results

Categories	Uncertainties (%)	Overall Uncertainty (%)
Turbulent Intensity	0.22%-0.45%	0.05%-0.90%
Static Temperature	0.15%-0.25%	
Heat of Reaction	0.55%-0.90 %	
Mass Fraction of CO_2, H_2O, and N_2	0.05%-0.07%	

The authors do believe that the experimental tests need to be done to further validate the results presented in this paper. The authors are still working on the project and aiming to perform the experimental tests soon.

4 Results and Discussions

This paper focuses on the CFD modeling of stoichiometric methane-air combustion (ϕ = 1) under a small-scale rectangular combustor at a wide range of methane and airflow conditions. The combustion study is performed using the species transport model (STM). To start the iteration in CFD, FV of 30 m/s (Re_{CH4} = 1.8 E+4) is considered as an arbitrary reference value. Then AV is changed from 2 m/s to 20 m/s (Re_{Air} = 3.2 E+4 to 3.2 E+5). This is how the optimum range of AV is decided. Similarly, to get the optimum range of FV, AV = 30 m/s (Re_{Air} = 4.9 E+5) is considered as an arbitrary reference value. The FV is changed from 2 m/s to 20 m/s (Re_{CH4}= 1.2 E+3 to 1.2 E+4). The authors are interested to present the flow and flame characteristics at low operating conditions first. After that, the flow and combustor behavior at moderate-to-high operating conditions will be discussed.

4.1 Flow and Flame Characteristics at Low Re_{Air} and Re_{CH4}

4.1.1 Flow and Flame Characteristics at Re_{Air} = 3.2 E+4 (AV = 2 m/s) when Re_{CH4} = 1.8 E+4 (FV = 30 m/s)

The flow inside a combustor is controlled by turbulence or diffusion. Also, the relative behavior of fluctuating velocity component over mean velocity is important for flow characterization. To address these, the turbulent intensities (I) are investigated. The turbulent intensity reaches a minimum of 4.2 (%) and a maximum of 700.1 (%) as shown in Fig. 3. The turbulent intensity is found to be around ~350% in the ignition zone. The higher turbulence in the ignition zone indicates better mixing and entrainment. The better mixing confirms the flame anchoring in the ignition zone.

The static temperature contour shows the instantaneous flame temperature of the methane-air combustion. As expected, the flame temperature reaches 2167 K at Re_{Air} = 3.2 E+4 (Fig. 4). It is seen that the temperature is well distributed inside the combustor. The flame expansion is seen to be high. The flame is expanded from the ignition point to the downstream direction. However, a better lateral expansion could be achieved if the flow swirl is further improved at the combustor inlet.

The heat released during the exothermic reaction defines the soundness of the combustion. To understand the heat transfer and overall heat generation, the heat of reaction contour is studied. In this case, the heat of reaction (ΔH) reaches a max of 15.2 W (Fig. 5). The thermal energy generation is maximized near the upstream of the combustor, especially in the mixing point or ignition point.

The study of mass fractions (mf) of the products is very important especially to determine the completeness of the combustion. The mass fraction of CO_2, H_2O, and N_2 are presented in Fig. 6. In the methane-air flame, the maximum mf_{CO2}, $mf_{H2O,}$ and mf_{N2} are found to be 0.142, 0.117, and 0.767 respectively. The mass fractions of the products are within the acceptable limits of CH_4-Air combustion as stated in [19]-[20]. Therefore, it is indicating that the combustion is complete and there is no unburn mixture present in the system.

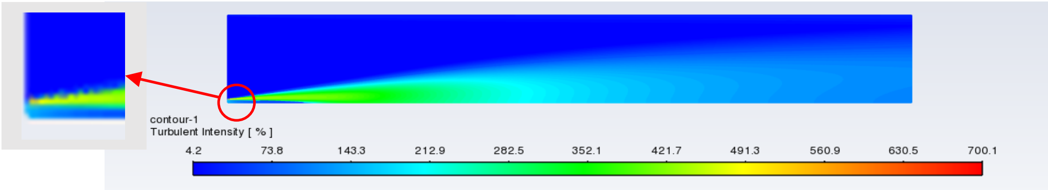

Fig. 3 Contour of the turbulent intensity at Re_{Air} = 3.2 E+4 (AV = 2 m/s)

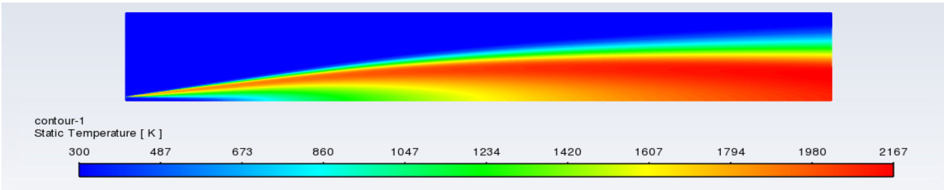

Fig. 4 Contour of the static temperature at Re_{Air} = 3.2 E+4 (AV = 2 m/s)

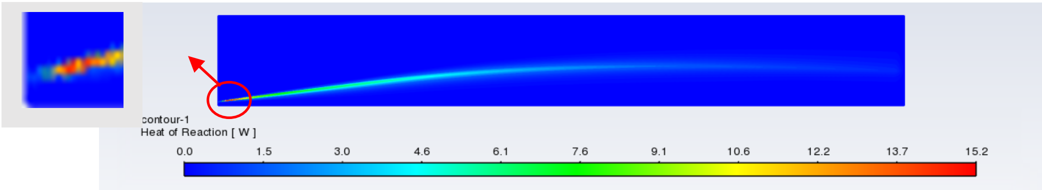

Fig. 5 Contour of heat of reaction during the methane-air combustion at Re_{Air} = 3.2 E+4 (AV = 2 m/s)

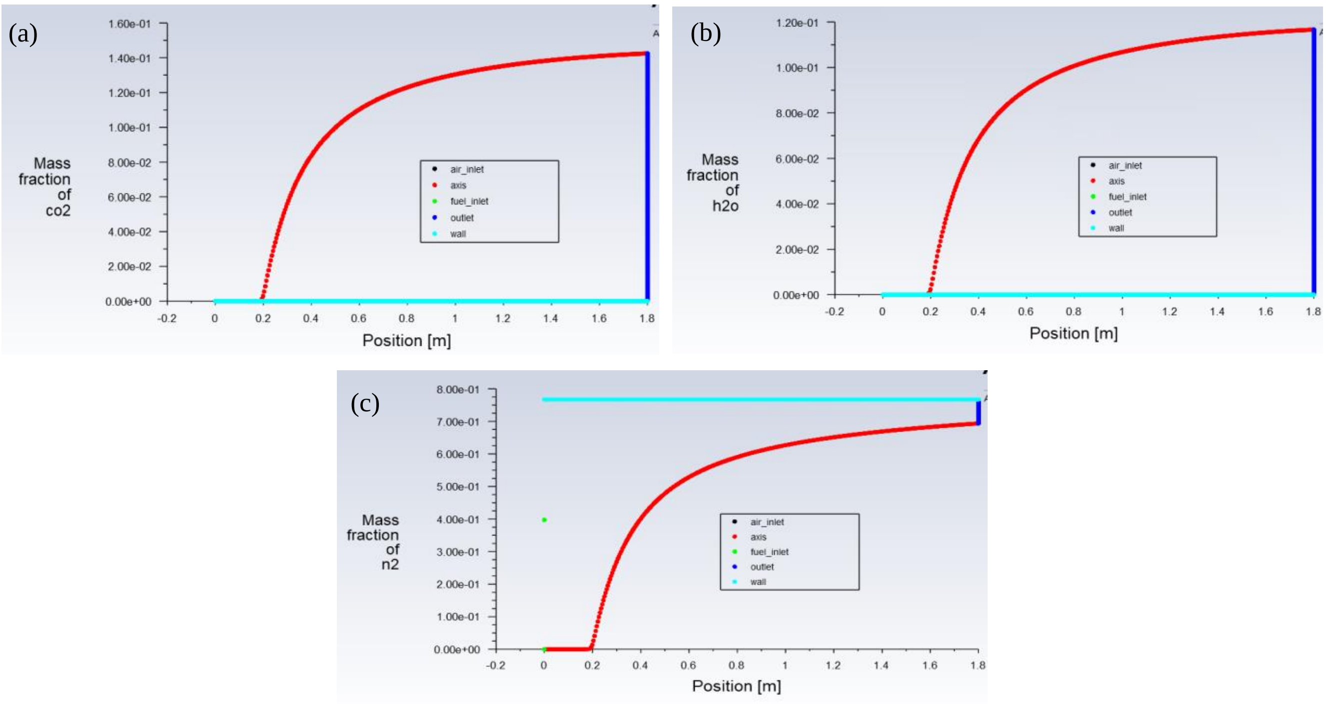

Fig. 6 Profiles of mass fraction of (a) CO_2, (b) H_2O and (c) N_2 at Re_{Air} = 3.2 E+4 (AV = 2 m/s)

4.1.2 Flow and Flame Characteristics at Re_{CH4} = 1.2 E+3 (FV = 2 m/s) when Re_{Air} = 4.9 E+5 (AV = 30 m/s)

The minimum and maximum turbulent intensity are found to be 10.0 % and 681 % respectively at Re_{CH4} = 1.2 E+3 (Fig. 7). The turbulent intensity is low compared to what is seen in Fig. 3. This is due to the low velocity (bulk) intake of the combustor. In another word, the relative change of velocity fluctuation over the average velocity is comparatively low in this case.

The static temperature reaches a maximum of 2269 K at Re_{CH4} = 1.2 E+3 (Fig. 8). It is also seen that at this specific condition, the flame is leaning to the bottom wall. This indicates that the flame has very little expansion or lateral displacement. It is due to the presence of less fluctuation or turbulence in the flow. Also, the recess length further needs to be checked so that fully burnt and expanded flame could be achieved even at high Re conditions. The heat of the reaction reaches 2.9 W (Fig. 9). The generation of heat (ΔH) is less in this case which is due to the intake of less fuel to the system.

The maximum mass Fraction of CO_2, H_2O, and N_2 reaches 0.146, 0.120, and 0.767 respectively (Fig. 10). The mass fraction of combustion products does not change with temporal and spatial directions. The mass fraction falls within the acceptable limits of CH_4-Air combustion, as stated in [19]-[20]. Thus combustion is considered to be complete.

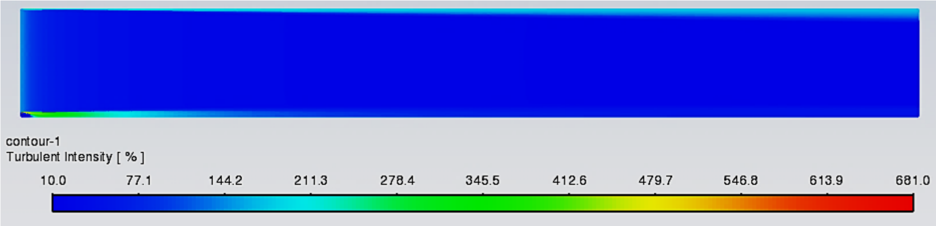

Fig. 7 Contour of the turbulent intensity at Re_{CH4} = 1.2 E+3 (FV =2 m/s)

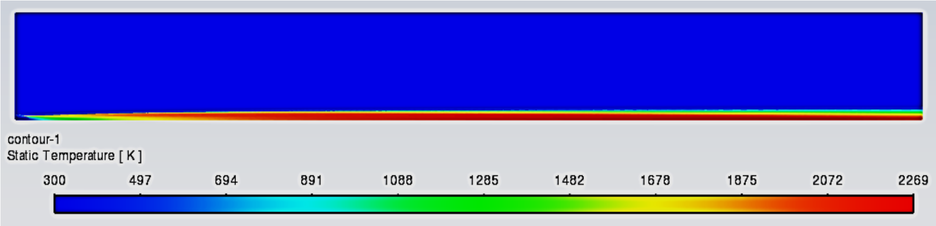

Fig. 8 Contour of the static temperature at Re_{CH4} = 1.2 E+3 (FV = 2 m/s)

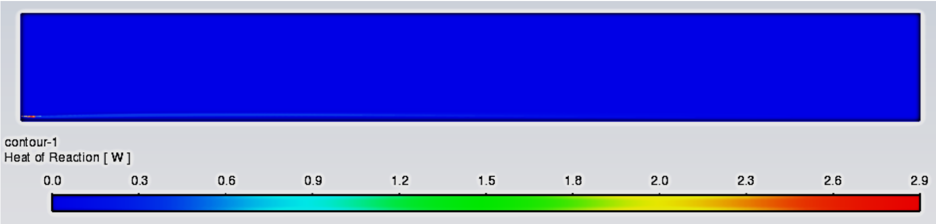

Fig. 9 Contour of heat of reaction at Re_{CH4} = 1.2 E+3 (FV = 2 m/s)

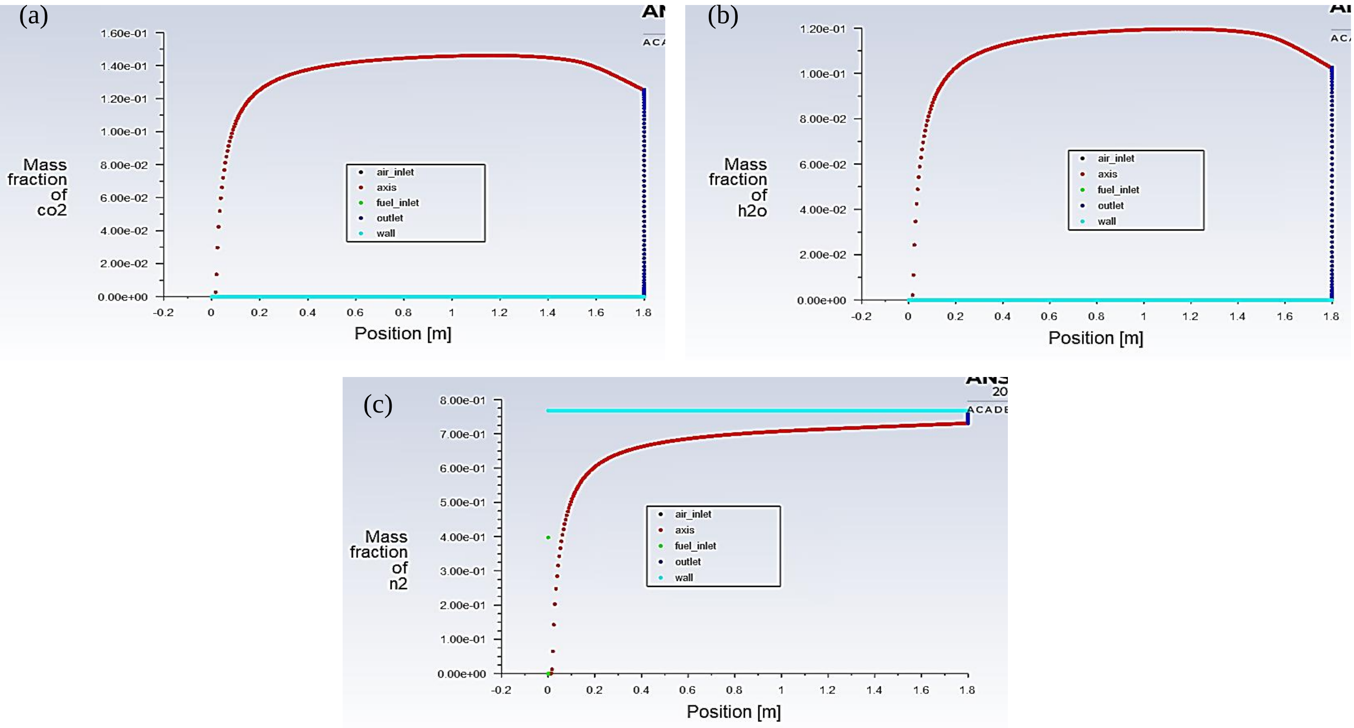

Fig. 10 Profiles of mass fraction of (a) CO_2, (b) H_2O and (c) N_2 at Re_{CH4} = 1.2 E+3 (FV = 2 m/s)

4.2 The Flow Properties and Combustion Dynamics at Variable Re_{Air}

The flow and combustion characteristics are investigated under AV = 4 m/s to 20 m/s (Re_{Air} = 6.5 E+4 to 3.2 E+5) while keeping Re_{CH4} = 1.8 E+4. It is observed from CFD analysis that going over AV = 14 m/s, does not provide stable and complete combustion. Thus the flow and combustion characteristics at Re_{Air} = 6.5 E+4 to 2.3 E+5 (AV = 4 m/s to 14 m/s) are only reported here.

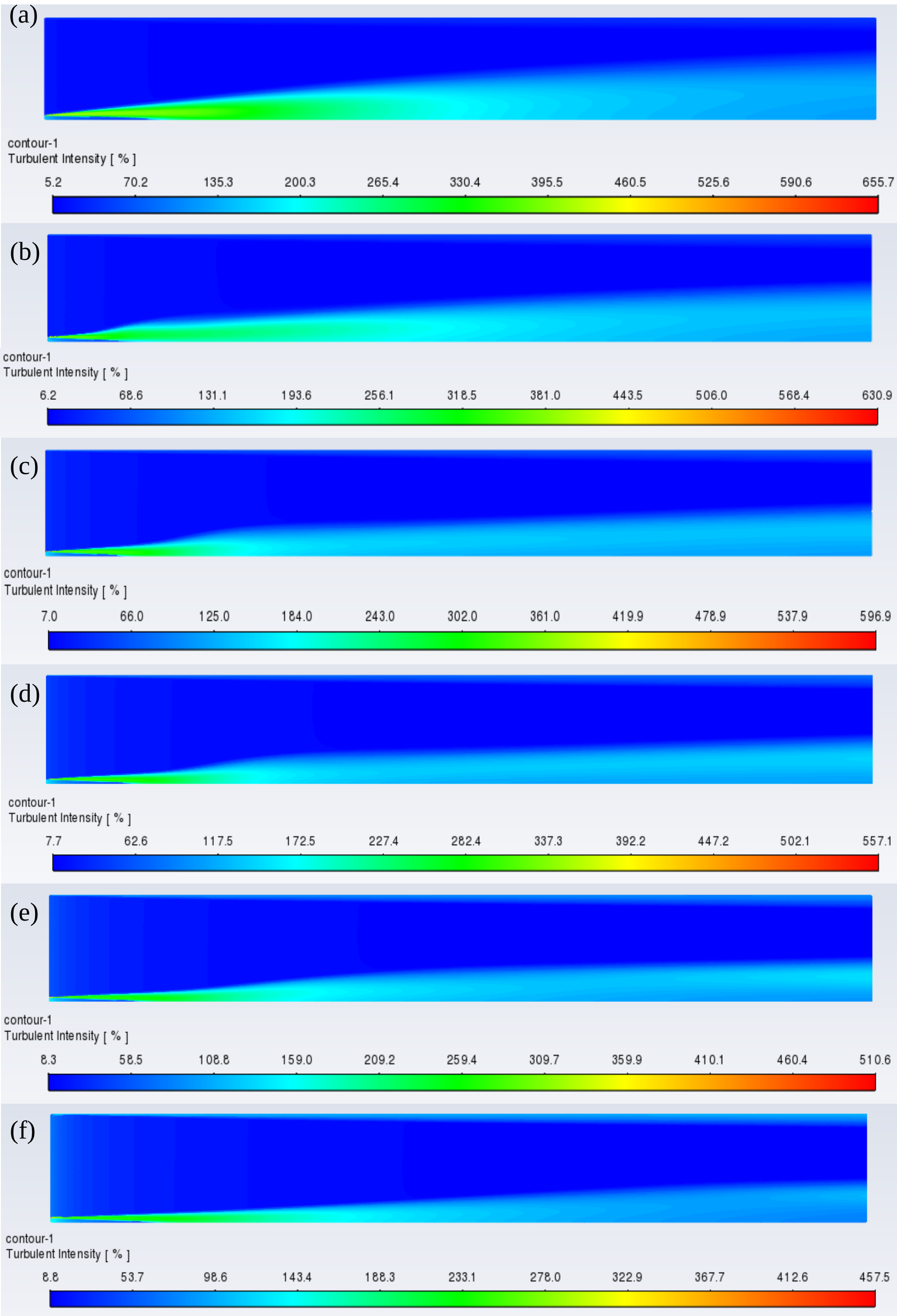

Fig. 11 The change in turbulent intensity contours at different Re_{air} values when Re_{CH4} is kept at 1.8 E+4, (a) Re_{air} = 6.5 E+4, (b) Re_{air} = 9.7 E+4 (c) Re_{air} = 1.3E+5, (d) Re_{air} = 1.6 E+5, (e) Re_{air} = 1.9 E+5, and (f) Re_{air} = 2.3 E+5

The turbulent intensity (I) increases with the increase in Re_{Air} (Fig. 11). The I_{min} increases from 5.2% to 8.8 % whereas I_{max} decreases from 655.7% to 457.5% as Re_{Air} changes from 6.5 E+4 (4 m/s) to 2.3 E+5 (14 m/s). Increasing AV positively affects the I_{min}, but adversely affects the I_{max} as long as MV remains constant. However, the overall turbulence value is high and sufficient enough to provide sound mixing in the combustor. The turbulence helps in flame anchoring in the ignition point. For future high Re (or Mach) testing, the decrease in flow turbulence might induce flame instability. The flow swirling ratio needs to be increased. The swirlers with different geometries or blunt bodies should be installed upstream of the combustor.

The static temperature decreases from 2153 K to 2013 K as Re_{Air} increases from 6.5 E+4 to 1.6 E+5. (Fig. 12 (a-d)). After that the static temperature increases to 2086 K and 2350 K when Re_{Air} = 1.9 E+5 and 2.3 E+5, respectively (Fig. 12 (e-f)). This sudden decrease and increase in static temperature could be correlated to the change in reactant entrainment rate, flow fluctuation, etc. Also, the mesh growth rate, mesh fining rate should be further checked to get a stable static temperature at these operating conditions. However, the change observed in static temperature (2013 K-2350 K) falls within the standard limit of methane-air combustion [19]-[20].

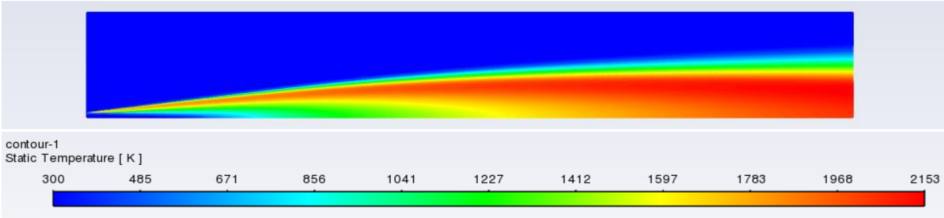

(a)

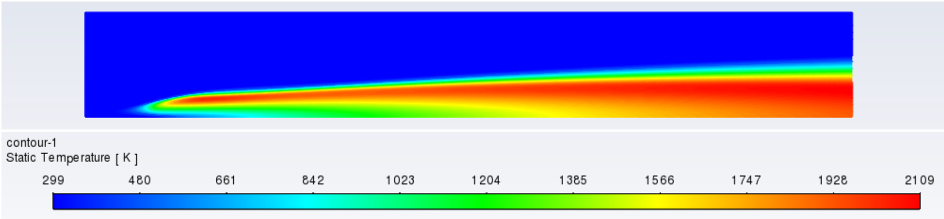

(b)

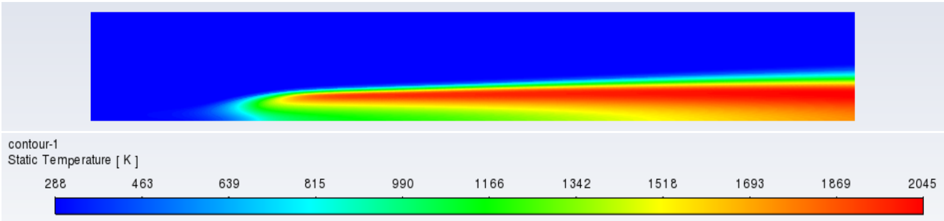

(c)

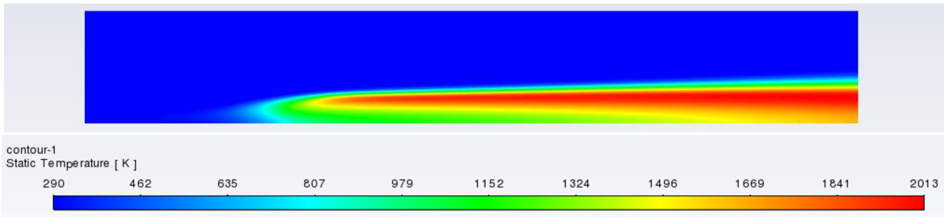

(d)

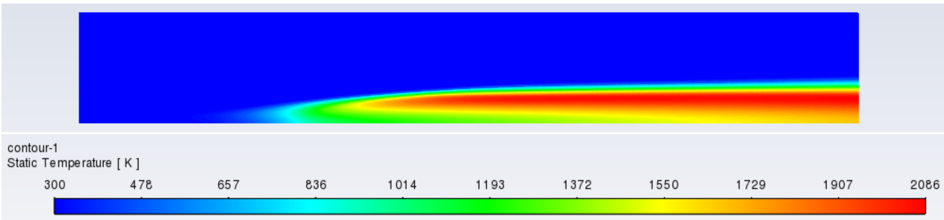

(e)

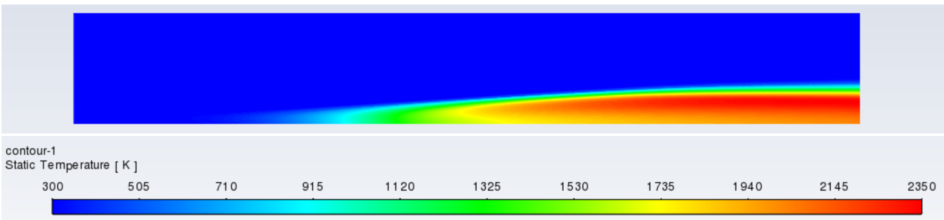

(f)

Fig. 12 The change in static temperature contours at different Re_{air} values when Re_{CH4} is kept at 1.8 E+4, (a) Re_{air} = 6.5 E+4, (b) Re_{air} = 9.7 E+4 (c) Re_{air} = 1.3E+5, (d) Re_{air} = 1.6 E+5, (e) Re_{air} = 1.9 E+5, and (f) Re_{air} = 2.3 E+5

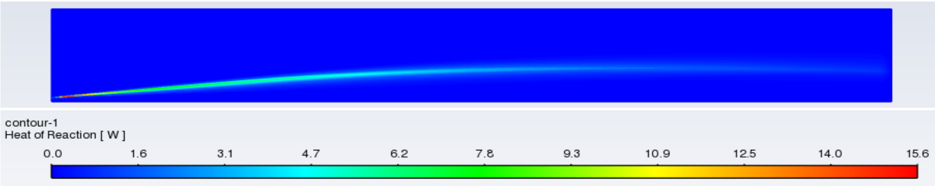

(a)

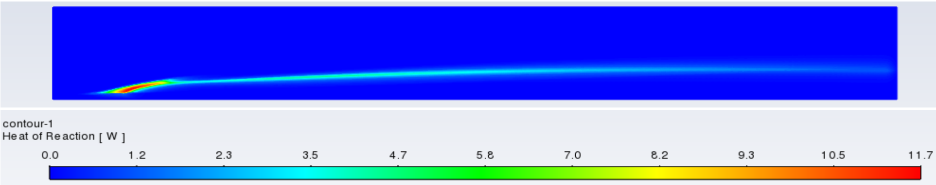

(b)

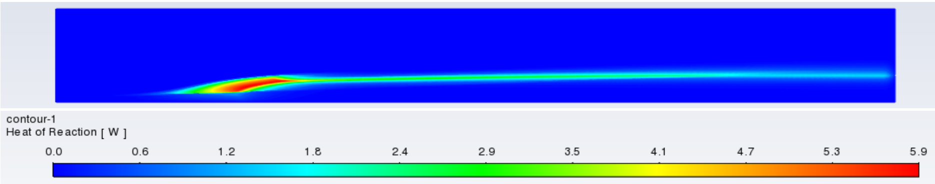

(c)

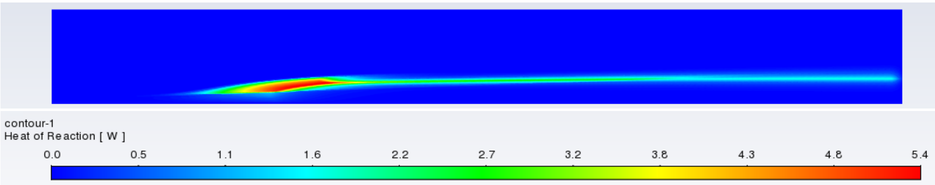

(d)

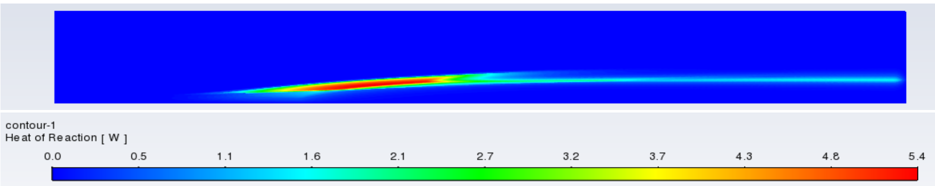

(e)

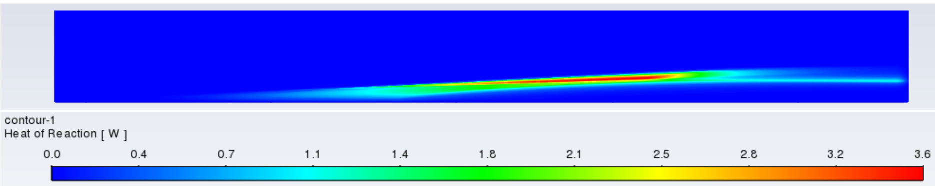

(f)

Fig. 13 The change in heat of reaction contours at different Re_{air} values when Re_{CH4} is kept at 1.8 E+4, (a) Re_{air} = 6.5 E+4, (b) Re_{air} = 9.7 E+4 (c) Re_{air} = 1.3E+5, (d) Re_{air} = 1.6 E+5, (e) Re_{air} = 1.9 E+5, and (f) Re_{air} = 2.3 E+5

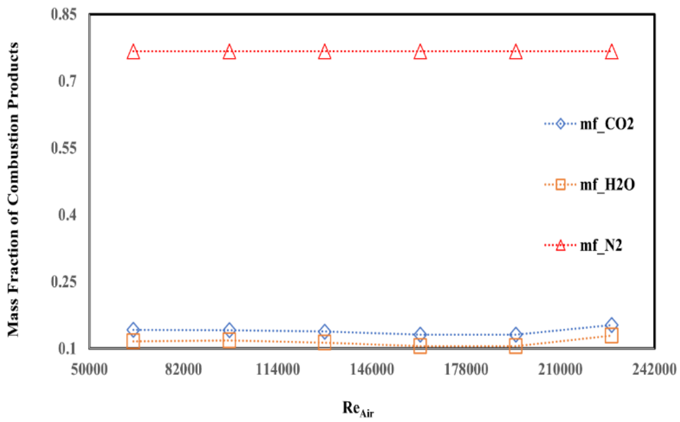

Fig. 14 The change in mass fraction of CO_2, H_2O and N_2 at different Re_{air} values when Re_{CH4} is kept at 1.8 E+4.

The heat of reaction (HOR) decreases from 15.6 W to 11.7 W as Re_{Air} increases from 6.5 E+4 to 9.7 E+4. (Fig. 13 (a-b)). After that, the HOR value remains constant at around ~5.5 W (Fig. 13 (c-d)). Then HOR drops to 3.6 W (Fig. 13 (f)). Overall HOR decreases with an increase in Re_{Air}. This decrease in heat generation is due to the insufficient supply of CH_4 in the system. The CH_4 supply should be adjusted (increased) to keep up the high level of HOR for each run of combustion tests. However, the heat of reaction magnitude is matched with the exothermic enthalpy of methane and air chemical reaction reported in [19]-[20]. The mass fraction of CO_2 at the combustor outlet decreases from 0.142 to 0.131 as Re_{Air} increases from 6.5 E+4 to 1.9 E+5 (Fig. 14). The mass fraction of CO_2 increases to 0.153 at Re_{Air} = 2.3 E+5 (Fig. 14). This increase in mass fraction of CO_2 should be further examined by increasing the meshing and relaxation factor in CFD. The mass fraction of H_2O decreases from 0.116 to 0.105 when Re_{Air} changes from 6.5 E+4 to 1.9 E+5 (Fig. 14). The mass fraction of H_2O increases to 0.129 at Re_{Air} = 2.3 E+5 (Fig. 14). The average mass fraction of H_2O is found to be 0.114 which is similar to what is stated in [19]. The mass fraction of N_2 at the combustor outlet remains constant at 0.767 when Re_{Air} changes from 6.5 E+4 to 2.3 E+5. The overall trend of mass fraction of CO_2, H_2O, and N_2 is steadier. The range of production mass fraction falls within the acceptable standard limit presented in [19].

4.3 The Flow Properties and Combustion Dynamics at Variable Re_{CH4}

The CFD investigation is further extended by keeping Re_{Air} constant at 4.9 E+5 (AV =30 m/s) and changing Re_{CH4} from 2.4 E+3 to 1.8 E+4 (FV = 4 m/s to 30 m/s). However, crossing over Re_{CH4} = 7.2 E+3 (MV =12 m/s), does not provide stable or complete combustion. Thus, the authors are interested to present the results at Re_{CH4} = 2.4 E+3 to 7.2 E+3 (MV = 4 m/s to 12 m/s) only. At this time, the effect of variable Re_{CH4} (at constant Re_{Air}) on the flame and flow properties is investigated. The minimum turbulent intensity (I_{min}) of ~12% is observed under all Re_{CH4} conditions. However maximum turbulent intensity (I_{max}) decreases from 667% to 524% as Re_{CH4} varies from 2.4 E+3 to 7.2 E+3 (Fig. 15). The decrease in I_{max} could be related to the presence of less flow fluctuation in the system. Installing swirlers or a bluff body upstream of the combustor could enhance the flow turbulence at high Reynolds conditions. Also, perforated plates with various blockage ratios could be used at the combustor inlet. The use of this kind of plate alters the turbulence level, eddy size, and overall flow fluctuation in the system.

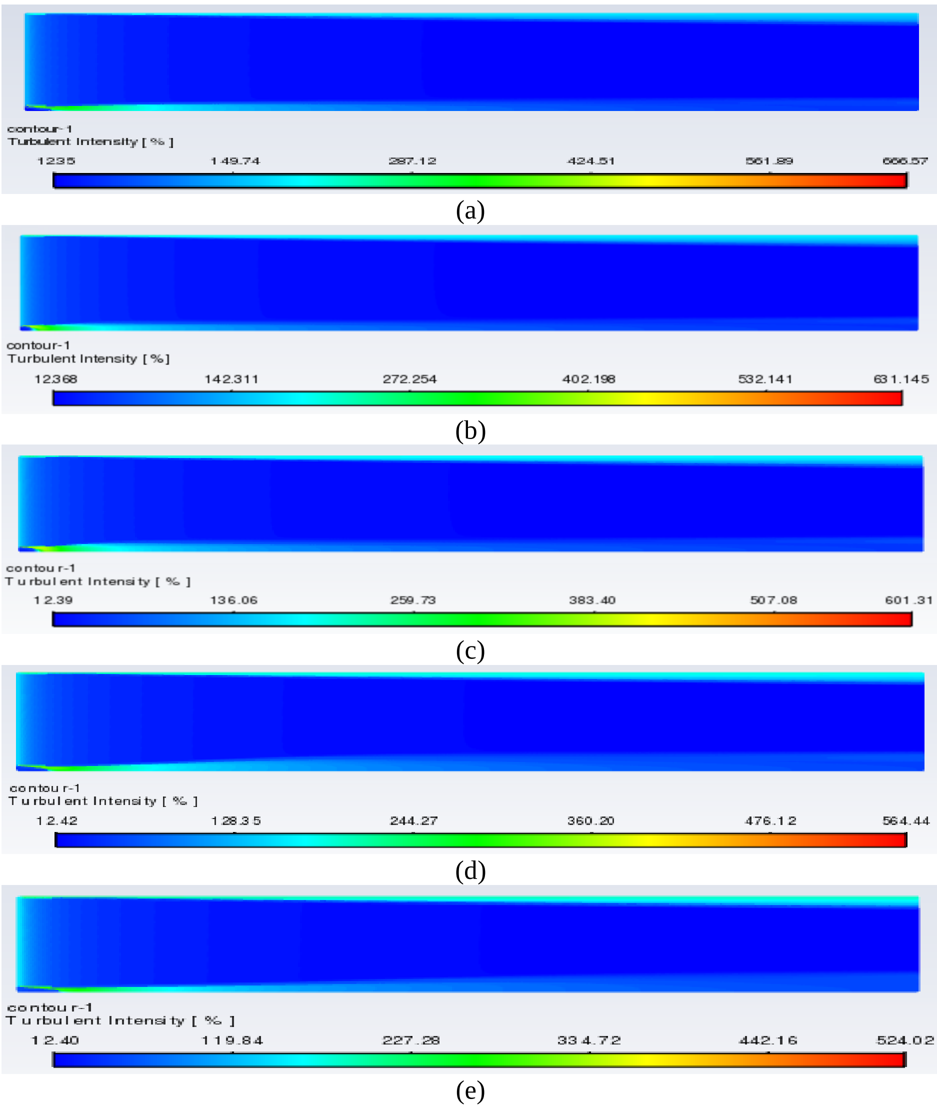

Fig. 15 Turbulent Intensity contour at variable Re_{CH4} when Re_{Air} is kept at 4.9 E+5, (a) Re_{CH4} = 2.4 E+3, (b) Re_{CH4} = 3.6 E+3 (c) Re_{CH4} = 4.8 E+3, (d) Re_{CH4} = 6.0 E+3, and (e) Re_{CH4} = 7.2 E+3

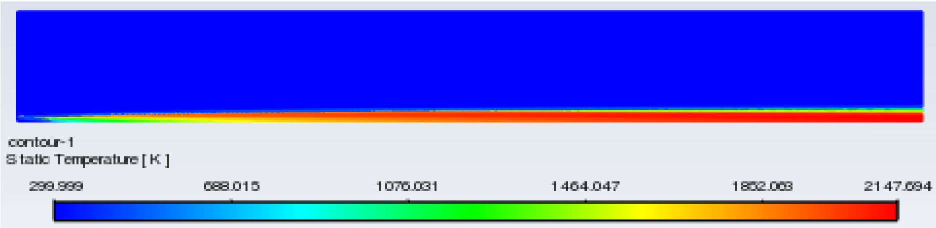

(a)

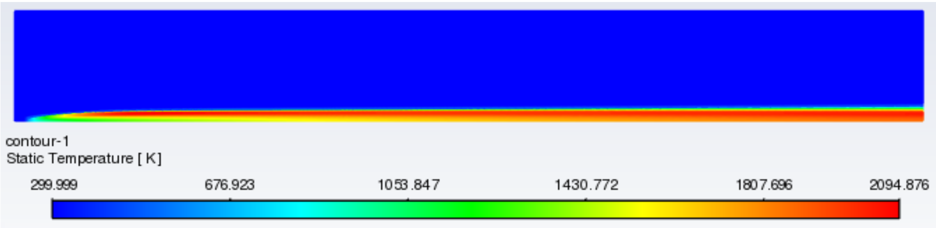

(b)

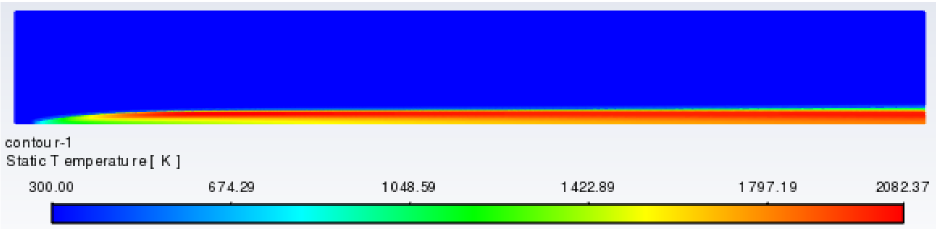

(c)

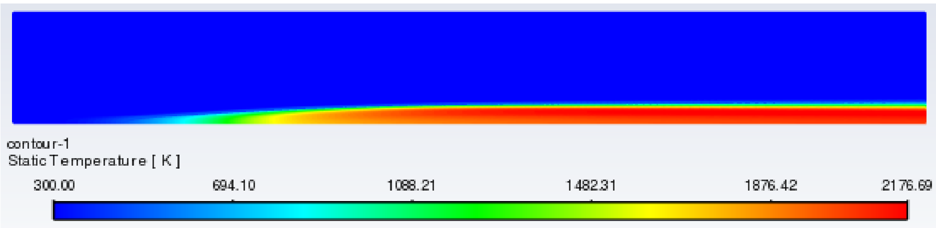

(d)

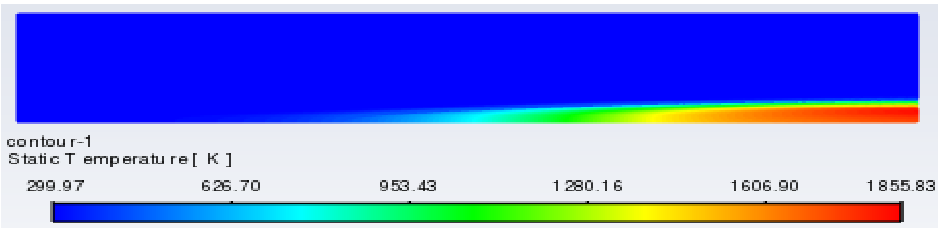

(e)

Fig. 16 The change in static temperature contour at variable Re_{CH4} when Re_{Air} is kept at 4.9 E+5, (a) Re_{CH4} = 2.4 E+3, (b) Re_{CH4} = 3.6 E+3 (c) Re_{CH4} = 4.8 E+3, (d) Re_{CH4} = 6.0 E+3, and (e) Re_{CH4} = 7.2 E+3

The static temperature decreases from 2148 K to 2082 K as Re_{CH4} varies from 2.4 E+3 to 4.8 E+3 (Fig. 16 (a-c)). The static temperature is then increased to 2177 K and decreased to 1856 K at Re_{CH4} = 6.0 E+3 and 7.2 E+3, respectively. The static temperature, in general, has decreased with the increase in Re_{CH4}. The decrease in static temperature results due to the insufficient supply of air into the combustor. Making the mixture oxygen-rich might mitigate this issue. In this research, only the stoichiometric mixture is considered. The authors do believe that the effect of different equivalence ratios (ϕ) or lean-to-rich mixture conditions at each Re should be investigated using both CFD and experiments.

The heat of reaction is found to be 3.0 at Re_{CH4} = 2.4 E+3 (Fig. 17 (a)), whereas it reaches a maximum of 8.9 and 8.1 at Re_{CH4} = 3.6 E+3 and 4.8 E+3, respectively (Fig. 17 (b-c)). The minimum heat of reactions of 1.3 and 1.2 are observed at Re_{CH4} = 6.0 E+3 and 7.2 E+3, respectively (Fig. 17 (d-e)). This change in heat of reaction is because of the constant supply of air while the methane velocity keeps changing. To overcome this, the air velocity needs to be adjusted at variable Re_{CH4}. A test matrix should be developed for air and methane flow velocities accommodating various equivalence ratios (ϕ).

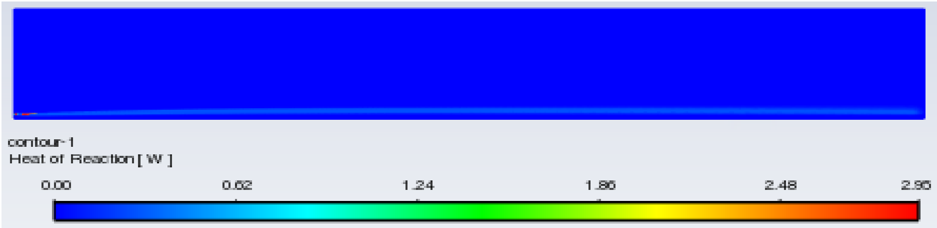

(a)

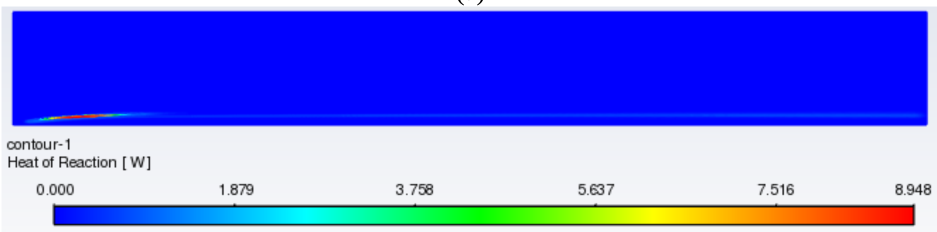

(b)

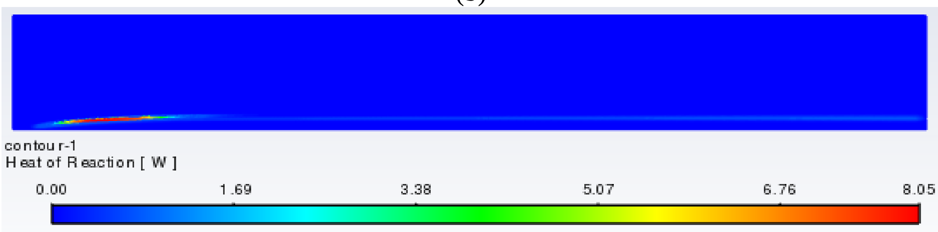

(c)

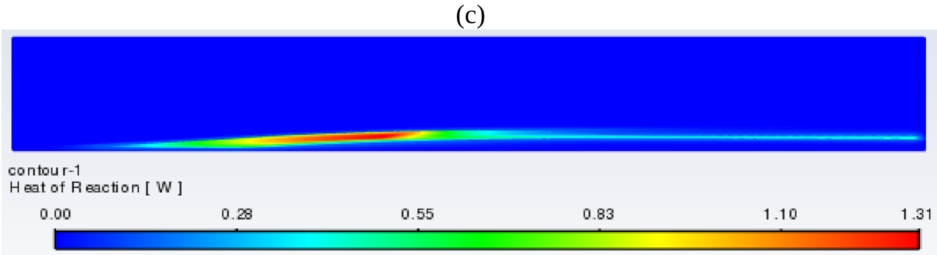

(d)

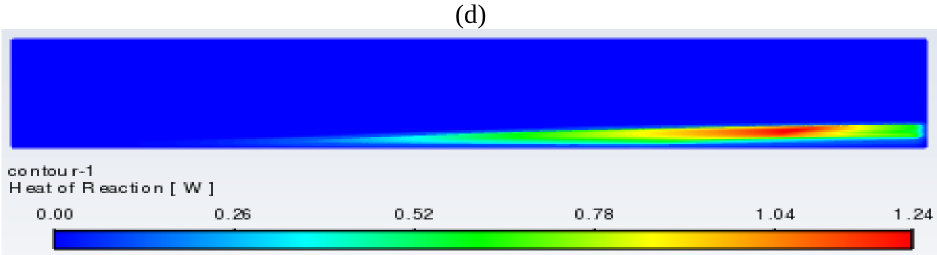

(e)

Fig. 17 The change in heat of reaction at variable Re_{CH4} when Re_{Air} is kept at 4.9 E+5, (a) Re_{CH4} = 2.4 E+3, (b) Re_{CH4} = 3.6 E+3 (c) Re_{CH4} = 4.8 E+3, (d) Re_{CH4} = 6.0 E+3, and (e) Re_{CH4} = 7.2 E+3

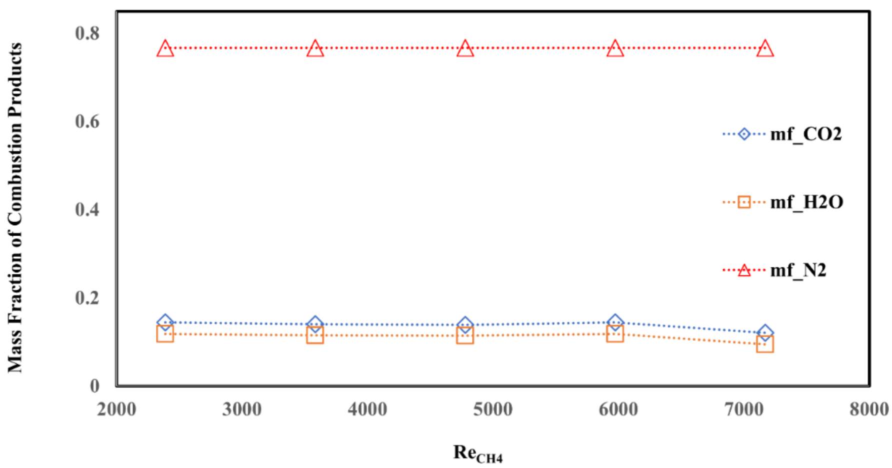

Fig. 18 The change in mass fraction of CO_2, H_2O and N_2 at variable Re_{CH4} when Re_{Air} is kept at 4.9 E+5.

The mass fraction of CO_2 decreases from 0.144 to 0.139 as Re_{CH4} increases from 2.4 E+3 to 4.8 E+3 (Fig. 18). The mass fraction reaches back to 0.144 at Re_{CH4} = 6.0 E+3 and again drops to 0.121 at Re_{CH4} = 7.2 E+3. There is a change in the mass fraction of CO_2, however, the change is not significant for most of the CFD runs. The mass fraction of H_2O decreases with the increase in Re_{CH4}. It decreases from 0.118 to 0.114 as Re_{CH4} changes from 2.4 E+3 to 4.8 E+3 (Fig. 18). After that, it reaches the original value of 0.118 and then drops to 0.095. An average mass fraction of H_2O of 0.112 is observed from the CFD study. The mass fraction of N_2 remains constant at 0.767 at all Re_{CH4} conditions. The mass fraction of products falls within the acceptable limit of CH_4-air combustion as reported elsewhere [19]-[20].

The ongoing research is focused on optimizing the possible test operating conditions for methane-air combustion under a small-scale rectangular combustor. In this research, a cross-validation technique has been implemented to develop an optimum test matrix. First, the fuel injection velocity is kept constant and air injection velocity is changed. The second time, the air injection velocity is kept constant and fuel injection velocity is changed. The authors found a preliminary test operating conditions: Re_{Air} and Re_{CH4} could be changed from 3.2 E+4 to 2.3 E+5 and 1.2 E+3 to 7.2 E+03, respectively. The authors are planning to continue this research using the reverse test validation method where at each of the fuel injection velocities, a wide range of air injection velocities will be investigated. Afterward, a complete test matrix will be proposed.

5 Conclusions

A species transport Model (STM) with 2D axisymmetric space is used to study the stoichiometric (ϕ =1) CH_4-Air combustion under an axisymmetric small-scale combustor. In this study, a parallel injection of methane and air streams is considered. The methane and air are introduced to the combustor without any prior mixing thus the mixture is non-premixed.

- The combustion and flow characteristics are investigated at air injection velocity (AV) = 2 m/s to 30 m/s and fuel injection velocity (FV) = 2 m/s to 30 m/s.
- The research shows that AV over 14 m/s and FV over 12 m/s do not provide stable and complete combustion. Thus, the authors come up with preliminary test operating conditions: Re_{Air} = 3.2 E+4 to 2.3 E+5 and Re_{CH4} = 1.2 E+3 to 7.2 E+3.
- In the first approach of CFD study, FV is kept at 30 m/s (Re_{CH4} =1.8 E+4) while AV is changed from 2 m/s to 14 m/s (Re_{Air} = 3.2 E+4 to 2.3 E+5). At these specific conditions, I_{min} increases from 5.2 % to 8.8 % whereas I_{max} decreases from 655.7 % to 457.5%. The static temperature varies from 2013 K to 2350 K. The heat of reaction (HOR) is decreased from 15.6 W to 3.6 W. The decrease in HOR value could be linked to the supply of less CH_4 into the combustor. The average mass fraction of the CO_2, H_2O, and N_2 are found to be 0.139, 0.115, and 0.767, respectively.
- In the second approach of the CFD study, a cross-test validation technique is implemented. Now, AV is kept at 30 m/s (Re_{Air} =4.9 E+5) while FV is changed from 2 m/s to 12 m/s (Re_{CH4} = 1.2 E+3 to 7.2 E+3). The I_{min} remains constant at ~12% whereas the I_{max} drops from 681% to 524 %. The static temperature varies between 1856 K and 2269 K. The heat of reaction (HOR) varies from 1.2 W to 8.9 W. The average mass fractions of CO_2, H_2O, and N_2 are 0.139, 0.113, and 0.767, respectively.
- The authors would like to conduct more research using combustion modeling, analytical analysis, and experimental tests. The authors are also interested to validate the CFD results with the experimental tests soon. The authors will investigate the effect of different equivalence ratios (ϕ) and Reynolds numbers on the flow and flame characteristics and see how that affects the combustor design.

Nomenclature

STM	Species Transport Model
AV	Airflow Velocity
FV	Fuel flow Velocity
μ_t	Turbulent Viscosity
D_t	Turbulent Diffusivity
TKE	Turbulent Kinetic Energy
G_b	Generation of TKE due to the Change in Buoyancy Forces
G_k	Generation of TKE due to the Change in Velocity Gradient
Y_i	The Local Mass Fraction of Each Species
σ_k, S_ε	Source terms used in Energy Transport Analysis
S_i	Rate of Creation by Particulate, Soot, etc.
R_i	Net Rate of Production of Species i by the Chemical Reaction
∇T	Change in Temperature during the Combustion
J_i	The Diffusion Flux of Species i
$D_{T,i}$	Coefficients of the Thermal Diffusion
$D_{i,m}$	Coefficients of the Mass Diffusion
Sc_t	The Turbulent Schmidt Numbers
ρ	Density of the reactants
k	Thermal Conductivity
C_p	Specific Heat
Re_{air}	Reynolds Number Based on Air Velocity and Air Inlet Slot Geometry
Re_{CH4}	Reynolds Number Based on Fuel Velocity and Fuel Slot Geometry
ϕ	Equivalence Ratio-a ratio of actual A/F ratio over stoichiometric A/F ratio

Acknowledgments

This research is not supported by any organizations or agencies. The authors would like to thank the Department of Mechanical Engineering and the IT team of Embry-Riddle Aeronautical University, Prescott, USA for providing access to the ANSYS 2021 R1 academic.

Declaration of Competing Interest

The authors declared that there are no known competing financial interests or personal relationships that could have appeared to influence the research work presented in this article.

References

[1] CO_2 Emissions from Fuel Combustion (2020 Edition) by *International Energy Agency (IEA), Accessed: 2021, Available:* http://energyatlas.iea.org/#!/tellmap/1378539487

[2] Hossain, M.A., 2020. Laser Diagnostics of Compressible and High-intensity Premixed Methane-air Combustion Inside a Backward Facing Step Combustor Using High-repetition Rate CH-PLIF and PIV (Doctoral dissertation, The University of Texas at El Paso).

[3] Islam, M.N.A., Hossain, M.A., De la Torre, M., Acosta-Zamora, A. and Choudhuri, A.R., 2019. Laser Diagnostics of Highly Turbulent Premixed Methane-Air Flow Over a

Backward Facing Step Using PIV and OH-PLIF. In *AIAA Propulsion and Energy 2019 Forum* (p. 4323).

[4] Hossain, M.A., Islam, M.N.A. and Choudhuri, A., 2019, July. Flame Imaging of Highly Turbulent Premixed Methane-Air Combustion Using Planar Laser Induced Fluorescence (PLIF) of CH (CX). In *ASME Power Conference* (Vol. 59100, p. V001T01A008). American Society of Mechanical Engineers.

[5] Hossain, M.A., Islam, M.N.A., Hossain, W. and Choudhuri, A.R., 2020. CH-PLIF Diagnostics of High Intensity Turbulent Premixed Methane-Air Combustion. In *AIAA Scitech 2020 Forum* (p. 1705).

[6] Hamzah, D.A., 2015. Theory Comparison between Propane and Methane Combustion inside the Furnace. *International Journal of Current Engineering and Technology*, *5*(4), pp.2429-2434.

[7] Ibrahim, I.A., Gad, H.M. and Shabaan, M.M., 2014. Numerical simulation of combustion characteristics of methane flame in an axisymmetric combustor model. *Global Journal of Engineering Science*, pp.2349-4506.

[8] Pitsch, H. and Peters, N., 1998. A consistent flamelet formulation for non-premixed combustion considering differential diffusion effects. *Combustion and flame*, *114*(1-2), pp.26-40.

[9] Matalon, M., 2007. Intrinsic flame instabilities in premixed and nonpremixed combustion. *Annu. Rev. Fluid Mech.*, *39*, pp.163-191.

[10] Lacaze, G. and Oefelein, J.C., 2012. A non-premixed combustion model based on flame structure analysis at supercritical pressures. *Combustion and Flame*, *159*(6), pp.2087-2103.

[11] Barths, H., Hasse, C. and Peters, N., 2000. Computational fluid dynamics modelling of non-premixed combustion in direct injection diesel engines. *International Journal of Engine Research*, *1*(3), pp.249-267.

[12] Hossain, M.A., December 2021. Study of Ultra Low-swirl Burner (LSB) for Non-Premixed Methane-Air Combustion Using Computational Analysis. Proceedings of the *International Conference on Mechanical Engineering and Renewable Energy 2021 (ICMERE 2021)*, 12 – 14, Chattogram, Bangladesh.

[13] Kassem, H.I., Saqr, K.M., Aly, H.S., Sies, M.M. and Wahid, M.A., 2011. Implementation of the eddy dissipation model of turbulent non-premixed combustion in OpenFOAM. *International Communications in Heat and Mass Transfer*, *38*(3), pp.363-367.

[14] Kongre, U.V. and Sunnapwar, V.K., 2010. CFD modeling and experimental validation of combustion in direct ignition engine fueled with diesel. *International Journal of Applied Engineering Research*, *1*(3), p.508.

[15] Enagi, I.I., Al-Attab, K.A. and Zainal, Z.A., 2017. Combustion chamber design and performance for micro gas turbine application. *Fuel Processing Technology*, *166*, pp.258-268.

[16] Davis, S.G., Joshi, A.V., Wang, H. and Egolfopoulos, F., 2005. An optimized kinetic model of H2/CO combustion. *Proceedings of the combustion Institute*, *30*(1), pp.1283-1292.

[17] D'Errico, G., Lucchini, T., Onorati, A. and Hardy, G., 2015. Computational fluid dynamics modeling of combustion in heavy-duty diesel engines. *International Journal of Engine Research*, *16*(1), pp.112-124.

[18] Hossain, M.A., 2022. Computational Study of Methane-air Combustion Using the Species Transport Model. In *AIAA SCITECH 2022 Forum* (p. 1102).

[19] Ge, H.W. and Gutheil, E., Modeling and Simulation of Turbulent Spray Flows Using RANS and PDF Transport Equations.

[20] Urzica, D. and Gutheil, E., 2008. Counterflow combustion modeling of CH4/air and CH4/O2 including detailed chemistry. *Italy: ILASS*.